0026-895X/08/7303-824–832$20.00
MOLECULAR PHARMACOLOGY
Copyright © 2008 The American Society for Pharmacology and Experimental Therapeutics
Mol Pharmacol 73:824–832, 2008

Vol. 73, No. 3
39081/3301055
Printed in U.S.A.

The Telomeric Protein TRF2 Is Critical for the Protection of A549 Cells from Both Telomere Erosion and DNA Double-Strand Breaks Driven by Salvicine

Yong-Wei Zhang, Zhi-Xiang Zhang, Ze-Hong Miao, and Jian Ding

Division of Anti-Tumor Pharmacology, State Key Laboratory of Drug Research, Shanghai Institute of Materia Medica, Chinese Academy of Sciences, Shanghai, People's Republic of China

Received June 15, 2007; accepted November 19, 2007

ABSTRACT

Telomere repeat binding factor 2 (TRF2) has been increasingly recognized to be involved in DNA damage response and telomere maintenance. Our previous report found that salvicine (SAL), a novel topoisomerase II poison, elicited DNA double-strand breaks and telomere erosion in separate experimental systems. However, it remains to be clarified whether they share a common response to these two events and in particular whether TRF2 is involved in this process. In this study, we found that SAL concurrently induced DNA double-strand breaks, telomeric DNA damage, and telomere erosion in lung carcinoma A549 cells. It was unexpected to find that SAL led to disruption of TRF2, independently of either its transcription or proteasome-mediated degradation. By overexpressing the full-length *trf2* gene and transfecting TRF2 small interfering RNAs, we showed that TRF2 protein protected both telomeric and genomic DNA from the SAL-elicited events. It is noteworthy that although both the Ataxia-telangiectasia-mutated (ATM) and the ATM- and Rad3-related (ATR) kinases responded to the SAL-induced DNA damages, only ATR was essential for the telomere erosion. The study also showed that the activated ATR augmented the SAL-triggered TRF2 disruption, whereas TRF2 reduction in turn enhanced ATR function. All of these findings suggest the emerging significance of TRF2 protecting both telomeric DNA and genomic DNA on the one hand and reveal the mutual modulation between ATR and TRF2 in sensing DNA damage signaling during cancer development on the other hand.

Telomere is the specialized ribonucleoprotein structure at the ends of chromosomes in eukaryotic cells, which specifically protects chromosomes from end fusion and genomic instability (Greider and Blackburn, 1996). Thus, telomere integrity in cells thus plays an essential role in the control of genomic stability. Dysfunction of telomeres leads to cell cycle arrest and initiates cell apoptosis or cell senescence (Lechel et al., 2005; Farazi et al., 2006; Herbig and Sedivy, 2006). Therefore, an increasing number of studies have focused on telomere maintenance.

Telomere maintenance depends heavily on telomere binding proteins, of which telomere repeat binding factor 2 (TRF2) is a critical member. TRF2 is one of six proteins consisting of the protein complex shelterin (de Lange, 2005). Shelterin has been shown to be located on telomeres and to be related to telomere length regulation and telomere structure maintenance (de Lange, 2005). However, recent reports have revealed that TRF2 is recruited to DNA double-strand break (DSB) sites immediately after DSBs take place (Bradshaw et al., 2005). The TRF2 protein is phosphorylated in response to DSB signals (Tanaka et al., 2005). Loss or mutation of TRF2 leads not only to telomeric structure destruction but also to DNA damage, apoptosis, or senescence concomitantly (van Steensel et al., 1998; Smogorzewska and de Lange, 2002; Wang et al., 2004; Lechel et al., 2005). In addition, TRF2 promotes the polymerization activity of DNA polymerase β on telomeric and nontelomeric DNA substrates (Muftuoglu et al., 2006). As such, TRF2 is emerging as a potential target in cancer therapy.

Salvicine (SAL) is a novel diterpenoid quinone compound synthesized by the structural modification of a natural product isolated from the Chinese medicinal herb *salvia prionitis*

This work was supported by the grants from the National Natural Sciences Foundation of China (30500618 and 30721005) and the Chinese Academy of Sciences (the special scientific research initiation fund for Z.-H.M., the winner of the Special Prize of the President Scholarship).

Article, publication date, and citation information can be found at http://molpharm.aspetjournals.org.

doi:10.1124/mol.107.039081.

ABBREVIATIONS: TRF2, telomere repeat binding factor 2; SAL, salvicine; ATM, ataxia-telangiectasia-mutated; ATR, ataxia-telangiectasia-mutated- and Rad3-related; DSB, double-strand break; ChIP, chromatin immunoprecipitation; siRNA, small interfering RNA; ppt, protein-DNA immunoprecipitate complex; PCR, polymerase chain reaction; RT-PCR, reverse-transcription polymerase chain reaction; MG-132, *N*-benzoyl-oxycarbonyl (*Z*)-Leu-Leu-leucinal; DMSO, dimethyl sulfoxide; FITC, fluorescein isothiocyanate; PBS, phosphate-buffered saline; DAPI, 4,6-diamidino-2-phenylindole; VP16, etopside; γ-H2AX, phosphorylated-H2AX; *A,* absorbance.

lance (Zhang et al., 1999). It is now undergoing its phase II clinical trials. SAL possesses potent in vitro and in vivo activities against malignant tumor cells (Qing et al., 1999) functioning as a noninteractive topoisomerase II poison (Meng et al., 2001a; Lu et al., 2005a,b). Moreover, SAL stimulates intracellular reactive oxygen species, which subsequently elicit DNA DSBs closely related with cell death (Lu et al., 2005b). Furthermore, SAL inhibits telomerase activity and shortens telomere length in a telomerase-independent manner (Liu et al., 2002, 2004). Because of the notion that the telomere erosion is critical for DNA DSBs, we have investigated whether tumor cells share the common response to telomeric and nontelomeric DNA damage upon exposure to salvicine. In particular, because TRF2 is increasingly recognized as being capable of functionally sensing DNA damage, we further investigated whether TRF2 is involved in salvicine-triggered telomere erosion and DNA DSBs.

The aim of the present study is to unravel the effect of SAL on genomic and telomeric DNA in a single system, to characterize the role of SAL on TRF2 expression, and to explore the possible involvement of TRF2 protein in SAL-driven events. This will hopefully further our understanding of the distinct or unidentified roles of TRF2 in cancer development.

Materials and Methods

Drugs and Chemicals. SAL was provided by the Department of Phytochemistry in the Shanghai Institute of *Materia Medica* of the Chinese Academy of Sciences. The purity of the compound was more than 99%. VP16 and caffeine were purchased from the Sigma Chemical Co. (St. Louis, MO). MG-132 was the product of the BIOMOL Research Laboratories (Plymouth Meeting, PA). Both SAL and VP16 were prepared at 100 mM in DMSO. Caffeine was dissolved at 80 mM in distilled water and then filtrated with a 0.22-μm filter (Millipore, Billerica, MA). MG-132 was dissolved at 20 mM in DMSO. The aliquots of SAL, VP16, and caffeine stock solutions were stored at −20°C, and MG-132 stock solution was kept in −80°C avoiding light. All drugs were diluted to desired concentrations in full medium immediately before each experiment. The final DMSO concentrations did not exceed 0.1%.

Cell Culture. A549 cells were obtained from the American Type Culture Collection (Manassas, VA) and cultured in Ham's F-12 medium (Invitrogen, Carlsbad, CA) supplemented with 10% (v/v) heat-inactivated fetal bovine serum (Invitrogen), 100 μg/ml streptomycin, 100 U/ml penicillin, and 2 mM L-glutamine in a humidified atmosphere (5% CO_2) at 37°C.

Comet Assays. DNA DSBs were evaluated using the neutral single-cell gel electrophoresis (neutral comet assays) as described previously (Olive et al., 1990) with minor modifications (Lu et al., 2005a). Quantification was performed by analyzing at least 50 randomly selected comets per slide with the Komet 5.5 software (Kinetic Imaging Ltd., Nottingham, UK). The Olive tail moment was selected as the parameter that best reflects the degree of DNA damage (arbitrary units, defined as the product of the percentage of DNA in the tail multiplied by the tail length), and the data were expressed as mean ± S.D.

Relative Telomere Length Assays. Relative telomere length was detected by flow cytometry (flow-FISH) via fluorescence in situ hybridization with a fluorescein-conjugated PNA probe using the Telomere PNA Kit/FITC for Flow Cytometry (Dako Denmark A/S, Glostrup, Denmark) according to the manufacturer's protocol with a slight modification (Liu et al., 2004). Relative telomere length was the ratio of the telomere fluorescence intensity in treated cells to that in the control; the telomere fluorescence intensity = (Mean FL1 with probe − mean FL1 without probe). The fluorescence intensity of the control cells was taken as 100%.

Telomere FISH and Terminal Deoxynucleotidyl Transferase dUTP Nick-End Labeling Assays. Cellular telomere signals and DNA break signals were detected with the Cy3-labeled telomere PNA probe and the FITC-labeled dUTP, respectively. Using the Telomere PNA FISH kit (Dako Denmark A/S), telomere signals were performed first. Cells were cultured and treated on chamber slides in six-well plates and then fixed in 4% paraformaldehyde in PBS for 15 min. After washing with PBS, the cells were permeabilized in 0.1% Triton X-100 for 10 min and washed again with PBS. The slides were immersed in the prehybridization solution for 10 min and subsequently in ice-cold ethanol series (70, 85, and 95%) and left in air until dried. Fifty microliters of terminal deoxynucleotidyl transferase dUTP nick-end labeling reaction mixture containing the FITC-labeled dUTP and terminal deoxynucleotidyl transferase (TdT) (Roche, Basel, Switzerland) was added to the slides. After incubation at 37°C for 1 h, the slides were washed three times with PBS, air-dried, and stained with 0.5 μg/ml DAPI for 30 min in the dark. Images were taken using a Leica TCS Confocal Microscope (Leica, Deerfield, IL).

Western Blot Analyses. Protein levels were measured by Western blotting with corresponding specific primary antibodies, including those against TRF2 (Imgenex, San Diego, CA), phosphorylated-H2AX (γ-H2AX) (Cell Signaling Technology, Danvers, MA), Ataxia-telangiectasia-mutated kinase (ATM) (Rockland Immunochemicals Inc., Rockland, ME), ATM- and Rad3-related (ATR) (Calbiochem, San Diego, CA), and Myc (Cell Signalling Technology, Danvers, MA). Shown are the representative data from separate experiments.

Immunofluorescence Assays. A549 cells plated on coverslips in 24-well plates were used to study the subcellular localization of TRF2 and γ-H2AX. Cells were air-dried, fixed for 30 min with 4% paraformaldehyde in PBS, pH 7.4, and washed twice with PBS. Then, the cells were incubated for 15 min with 0.2% Triton X-100 and washed with PBS. After that, the cells were incubated in blocking buffer (3% bovine serum albumin in PBS) for 30 min before being incubated for 1 h with the primary antibodies against TRF2 (Imgenex) and γ-H2AX (Cell Signaling Technology). After three washes (2 min each) with PBS, the cells were incubated for an additional 1 h with the Alexa Fluor 488-conjugated secondary antibody (Alexa Fluor 488 goat anti-mouse IgG; Invitrogen). The cells were washed three times and stained with 0.5 μg/ml 4,6-diamidino-2-phenylindole for 30 min in the dark. Images were taken using a Leica TCS Confocal Microscope (Leica). Fluorescence was semiquantitated by Photoshop 7.0 software (Adobe Systems, Mountain View, CA).

RNA Extraction and RT-PCR. Total cellular RNA was isolated from A549 cells with the RNeasy Mini Kit (QIAGEN, Hilden, Germany) using the standard protocol for animal cells. The semiquantitative reverse transcription-PCR (RT-PCR) for *trf2* mRNA was performed with the QIAGEN OneStep RT-PCR Kit. *Trf2* primers used were 5′-TCC CAA AGT ACC CAA AGG C-3′ (sense) and 5′-ACT CCA GCC TTG ACC CAC TC-3′ (antisense). Glyceraldehyde-3-phosphate dehydrogenase was used as the loading control with the primers of 5′-TCA CCA TCT TCC AGG AGC GAG A-3′ (sense) and 5′-GCA GGA GGC ATT GCT GAT GAT C-3′ (antisense). The One-Step RT-PCR program was run as follows: for the reverse transcription, 50°C for 30 min and 95°C for 15 min; and for the PCR, hot start 94°C for 2 min followed by 36 cycles of 94°C for 30 s, 60°C for 30 s and 72°C for 45 s, and then 72°C, 10 min. The PCR products were resolved by 1.5% agarose electrophoresis.

Telomere-ChIP. ChIP was carried out using a chromatin IP (ChIP) assay kit, following the manufacturer's instructions (Millipore, Billerica, MA). Cells were fixed with formaldehyde for 10 min and then sonicated. Sonicated samples were precleared and precipitated with the TRF2 antibody (Imgenex). The resulting precipitates (ppt) were blotted onto a Hybond-N membrane (GE Healthcare, Chalfont St. Giles, Buckinghamshire, UK) under vacuum. Aliquots

of the supernatants before immunoprecipitation were taken out as inputs. Telomere repeat sequences were detected with a TeloTAGGG telomere length assay kit (Roche Diagnostics). In brief, the membrane was hybridized with a DIG-labeled telomere probe. The hybridized telomeric DNA was probed with the anti-DIG antibody. Telomere signals were semiquantitated with InGenius Bio-Imaging System (Syngene, Cambridge, UK). Telomeric DNA in ChIP (as a percentage) = telomeric DNA signal of ppt/telomeric DNA signal of input × 100%.

Construction of Recombinant Expression Plasmids. *pCDNA3.1-myc-his(−)A- trf2* and *pCDNA3.1-myc-his(−)A-trf2*$^{\Delta B\Delta M}$. *pBabe puro-trf2* and *pBabe puro-trf2*$^{\Delta B\Delta M}$ were taken as the template plasmids, which were kind gifts from Professor de Lange Titia in the Rockfeller University (New York, NY). The full-length *trf2* gene was amplified by PCR with two primers carrying EcoRI and BamHI sites: 5′-GTG CTG GAT ATC TGC AGA ATT CCA ATG GCG GGA GGA GGC GGG AGT AGC G-3′ (sense) and 5′-CTT GGT ACC GAG CTC GGA TCC GTT CAT GCC AAG TCT TTT CAT GGT CCG CC-3′ (antisense). The *trf2*$^{\Delta B\Delta M}$ PCR primers with EcoRI and BamHI sites used for amplification were 5′-GTG CTG GAT ATC TGC AGA ATT CCA ATG GAG GCA CGG CTG GAA GAG GCA GTC A-3′ (sense) and 5′-CTT GGT ACC GAG CTC GGA TCC TTC TAC AGT CCA CTT CTG CTT TTT TGT TA-3′ (antisense). Eighty nanograms of template plasmids was added to a 50-μl PCR system, including 1× buffer (10 mM Tris-HCl, pH 8.3, 1.5 mM $MgCl_2$, and 50 mM KCl), 50 μM dNTPs, 3 units of *Taq*DNA polymerase, and 0.1 μM concentration of specific primers. The PCR mixture was subjected to 30 cycles of 94°C for 30 s, 55°C for 30 s, and 72°C for 1 min. The amplified products were digested with EcoRI and BamHI and ligated to the corresponding cloning sites in the *pcDNA3.1/myc-His(−)A* mammalian expression vector (Invitrogen).

Transfection of Plasmids and Selection for Stable Expression Cell Lines. The plasmids were transfected with Lipofectamine 2000 (Invitrogen). For each transfection, 4 μl of Lipofectamine 2000 was added to 200 μl of Opti-MEM and incubated at room temperature for 5 min. The mixture was then added to further 200 μl of Opti-MEM with 2 μg of plasmid DNA for 20 min. The transfection complexes were then applied to cells within 600 μl of Opti-MEM medium. After 4-h incubation, 1 ml of fresh F-12 medium was added to the cells. Twenty-four hours later, the medium was replaced with fresh full medium. Thereafter, positive transefected cells were selected with 500 μg/ml G418. The Myc tag was detected by Western blotting.

Small Interfering RNA and Transfection. Three pairs of TRF2 small interfering RNA (siRNA) sequences were designed as number 1, 5′-CCU UCU UUA GUG GUU UGC UUA UdTdT-3′ (sense) and 5′-AUA AGC AAA CCA CUA AAG AAG GdTdT-3′ (antisense); number 2, 5′-ACC UAA UUU CAU UCU UUG UGA AdTdT-3′ (sense) and 5′- UUC ACA AAG AAU GAA AUU AGG UdTdT-3′ (antisense); and number 3, 5′-CGG CUU UCA UUU CCA CAG AAU UdTdT-3′ (sense) and 5′-AAU UCU GUG GAA AUG AAA GCC GdTdT-3′ (antisense). Their target sequences are all located within the 3′-UTR region of the TRF2 cDNA (no. 1, nucleotides 2199–2220; no. 2, nucleotides 2702–2723; no. 3, nucleotides 1633–1653). ATR siRNA sequences were 5′-CCU CCG UGA UGU UGC UUG AdTdT-3′ (sense) and 5′-UCA AGC AAC AUC ACG GAG GdTdT-3′ (antisense) (Casper et al., 2002). ATM siRNA sequences were 5′-CAU ACU ACU CAA AGA CAU UdTdT-3′ (sense) and 5′-AAU GUC UUU GAG UAG UAU GdTdT-3′ (antisense) (Nur-E-Kamal et al., 2003). All of the RNA oligonucleotides and the mock siRNAs were synthesized by the Genepharma Co. (Shanghai, China). siRNAs were transfected with the Oligofectamine reagent (Invitrogen) according to the manufacturer's instructions.

Sulforhodamine B Assays. The sensitivity of A549 cells to SAL was evaluated by sulforhodamine B assays (Lu et al., 2005a). The cell proliferation inhibition rate was calculated as proliferation inhibition (as a percentage) = $[1 - (A_{515\ \text{treated}}/A_{515\ \text{control}})] \times 100\%$.

In Vitro Assays for ATR Kinase Activity. ATR kinase assays with immunoprecipitated ATR from A549 cells were carried out as described previously (Canman et al., 1998) with minor modifications. After treatment, cells were trypsinized and washed three times in ice-cold PBS, and the pellets were lysed for 10 min at 4°C in 200 μl of lysis buffer (25 mM HEPES, pH 7.4, 300 mM NaCl, 5 mM EGTA, 1 mM $MgCl_2$, 0.5% Nonidet P-40, 10 μg/ml aprotinin, 1 μg/ml pepstatin A, 10 μg/ml leupeptin, 2 mM phenylmethylsulfonyl fluoride, 20 nM microcystin-LR, and 25 mM NaF). Precleared lysates were incubated with the ATR primary antibody (Calbiochem) and protein A/G agarose at 4°C overnight. The complexes were washed three times with lysis buffer and then twice with kinase reaction buffer (50 mM HEPES, pH 8.0, 10 mM $MnCl_2$, 2.5 mM EDTA, and 1 mM dithiothreitol). The beads were then resuspended in 30 μl of kinase reaction buffer containing 10 mM ATP and 5 μg of p53 recombinant protein (LabVision Corporation, Fremont, CA). The mixture was incubated at 30°C for 30 min. Then, 30 μl of 2× SDS loading buffer was added, and the phosphorylated proteins were separated by SDS-polyacrylamide gel electrophoresis, then normal Western blotting proceeded with the anti-phospho-p53(Ser15) antibody (Cell Signaling). Bands of phospho-p53 were scanned and semiquantitated with the InGenius Bio-Imaging System (Syngene, Cambridge, UK). The activity of ATR in the mock-siRNA-alone group was taken as 100%.

Statistical Analyses. All the data are represented as mean values ± S.D. The significance of differences between means was assessed by Student's *t* test, with $P < 0.05$ and $P < 0.01$ considered statistically significant.

Results

SAL Induced both DNA DSBs and Telomeric Erosion in A549 Cells. To detect whether SAL concurrently induces both DNA DSBs and telomeric erosion, we treated A549 cells with different concentrations of SAL for 3 h. Using comet assays, we found that SAL elicited DNA DSBs as shown by "comet tails" in neutral electrophoresis (Fig. 1A). The degree of DNA DSBs was augmented as the concentrations of SAL increased (Fig. 1A). The increase of the γ-H2AX level and the formation of γ-H2AX foci in the SAL-treated A549 cells further confirmed the result from comet assays (Fig. 1B). These data indicated that SAL produced genomic DSBs and activated a DNA damage response in A549 cells.

At the same time, SAL also damaged and shortened telomeric DNA. Using the telomere-specific probe and dUTP-FITC to label telomeric DNA and DNA breaks, respectively, their colocalization was defined as DNA break foci at telomere sites (Karlseder et al., 2004; Bradshaw et al., 2005). From Fig. 1C, the colocalization of DNA break signals and telomere signals appeared in the cells treated with 25 μM SAL. With increasing concentrations of SAL, DNA breaks were observed across the nuclei in a diffuse pattern, and DNA damage at telomere sites increased concurrently. Moreover, as the concentrations of SAL increased from 25 to 100 μM, the relative telomere length reduced progressively from 87.7 ± 6.6 to 53 ± 1.5% (Fig. 1D). The data above demonstrated that SAL could induce both telomeric and nontelomeric DNA damage in A549 cells.

SAL Disrupted TRF2 Protein in A549 Cells. TRF2 protein has been shown to bind to telomeric DNA and protects the structure of telomeres (Stansel et al., 2001; Yoshimura et al., 2004). Release of TRF2 from telomeres leaves the telomeric DNA unprotected (Li et al., 2005). In addition, TRF2 has also been suggested to be related to nontelomeric DNA damage and DNA repair events (Bradshaw et al., 2005; Tanaka et al., 2005; Muftuoglu et al., 2006). Using immunofluorescence microscopy, dot blotting, and

Western blotting, we found that SAL dramatically reduced the TRF2 protein levels in A549 cells (Fig. 2A). However, the levels of *trf2* mRNA did not change before and after SAL treatment (Fig. 2B, top). The proteasome inhibitor MG-132 also could not reverse the SAL-induced down-regulation of TRF2 protein, although MG-132 apparently enhanced the level of hypoxia-induction factor 1α, which is known to be degraded via the proteasome pathway (Li et al., 2004) (Fig. 2B, bottom). Therefore, such reduction in TRF2 protein was irrelevant to TRF2 transcription or to TRF2 degradation via the proteasome pathway (Fig. 2B). We further detected the ratio of the telomeric DNA bound to TRF2 relative to the total telomeric DNA using telomere-ChIP assays. SAL was shown to significantly decrease the telomeric DNA bound to TRF2, from 83.6 ± 2.4 to 48.7 ± 1% (Fig. 2C), indicating that some TRF2 was released from telomeric DNA. The data above suggested that SAL was likely to potentiate damage to telomeric and genomic DNA by disrupting the protection mechanism based on TRF2 protein.

TRF2 Attenuated SAL-Induced DNA Damage and Telomere Erosion. To clarify the involvement of TRF2 to SAL-elicited DNA damage events, we overexpressed TRF2 and down-regulated TRF2 expression using its siRNAs. The myc-tagged full-length *trf2* constructs and the basic/myb domain double-deficient *trf2-bm* constructs (van Steensel et al., 1998) were transfected into A549 cells and overexpressed effectively (Fig. 3A). Comet assays (Fig. 3B) and γ-H2AX detection (Fig. 3C) showed that the full-length *trf2* transfection produced fewer DSBs and lower levels of γ-H2AX in A549 cells after the treatment with SAL compared with the vector transfection. Moreover, the telomere shortening (Fig. 3D) and cytotoxicity (Fig. 3E) induced by SAL were also rescued by the full-length *trf2* transfection. In contrast, the double-deficient *trf2-bm* transfection, which exerts a dominant-negative-like action (van Steensel et al., 1998; Smogorzewska and de Lange, 2002), enhanced the genotoxic effects of SAL (Fig. 3, B–E). These data showed that overexpression of TRF2 could protect cells from SAL-induced DNA damage and telomere erosion.

On the other hand, we detected the effects of three TRF2 siRNAs with different sequences in A549 cells. All of the target sequences are located in the 3′-UTR of *trf2* gene. Among them, the no. 2 TRF2 siRNA elicited the most prominent down-regulation of TRF2 expression 24 h after transfection (Fig. 3F) and was chosen for the subsequent experiments. The TRF2 siRNA transfection resulted in higher levels of γ-H2AX (Fig. 3G) and more severe erosion of telomeres (Fig. 3H) induced by SAL than the mock siRNA transfection. Our results indicated that the reduction of TRF2

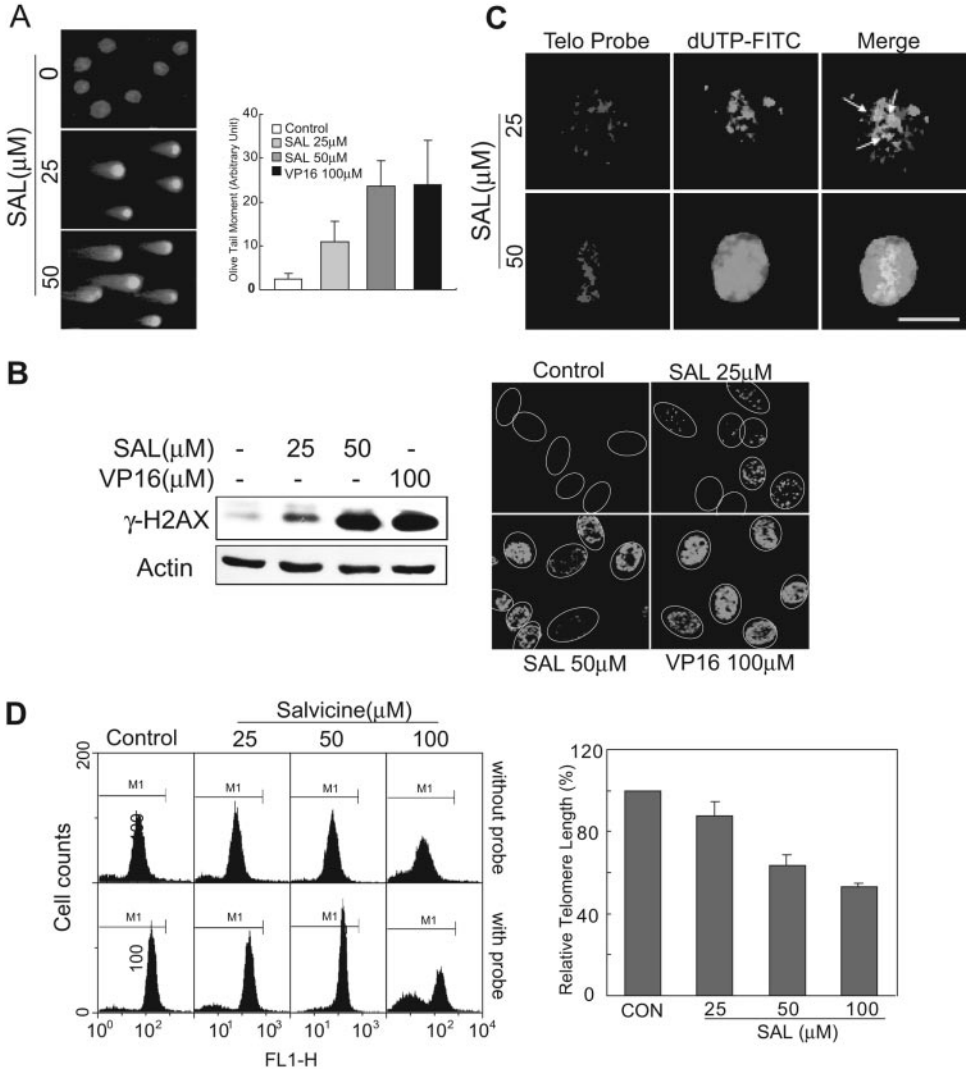

Fig. 1. SAL concurrently induces DNA double-strand breaks and telomeric erosion. A, A549 cells were treated with 25 or 50 μM SAL or 100 μM VP16 for 3 h and were harvested for detection of DNA DSBs by neutral comet assays. Representative "comet" images (200×, left) from three separate experiments are shown in which DNA was stained with DAPI. Results were semiquantitated with the Komet 5.5 software and expressed as the Olive tail moment (right). B, phosphorylation of γ-H2AX in the SAL-treated A549 cells. Left, the levels of γ-H2AX protein detected by Western blotting; right, formation of γ-H2AX foci examined by immunofluorescence confocal microscopy. Nuclear outlines were superimposed using the respective DAPI images. C, the damage sites on telomeric DNA. A549 cells were treated with 25 or 50 μM SAL for 3 h. Telomere signals were detected with a Cy3-labeled telomere PNA probe; DNA breaks were presented with FITC-labeled dUTP. The DNA break sites colocalized with the telomeres after SAL treatment (right), bar = 5 μm. D, telomere shortening was induced by SAL. Telomere length was detected by flow-FISH with a fluorescein-conjugated PNA probe. Representative histograms of flow cytometry from three independent experiments (left) were revealed. Relative telomere length was expressed as mean ± S.D. (right). Relative telomere length was the ratio of the telomere fluorescence intensity in treated cells to that in the control; the telomere fluorescence intensity = (Mean FL1 with probe − mean FL1 without probe). The fluorescence intensity of the control was taken as 100%.

potentiated DNA DSBs and telomere shortening in response to genotoxic stress. Taken together, our data from TRF2 overexpression and down-regulation experiments suggested that TRF2 protein provided cells abilities to prevent telomeric and nontelomeric DNA from genotoxic insults with a protection mechanism.

The DNA Damage Sensor ATR Was Required for the Cellular Response to the SAL-Induced DNA Damage and Telomere Shortening. TRF2 has been suggested to be coupled with DNA damage response (Bradshaw et al., 2005; Tanaka et al., 2005). The protein kinases ATM and ATR are two key sensors for DNA damage signaling (McGowan and Russell, 2004). To investigate how TRF2 protein is involved in DNA damage events after SAL exposure, we first detected whether ATM and ATR function in the SAL-induced DNA damage. Caffeine, an inhibitor for both ATM and ATR (Blasina et al., 1999; Sarkaria et al., 1999; Zhou et al., 2000), nearly eliminated SAL-induced γ-H2AX (Fig. 4A) and completely rescued telomeres from SAL-induced erosion (Fig. 4D). However, only the down-regulation of ATR with siRNA totally prevented the SAL-induced H2AX phosphorylation and telomere erosion in A549 cells (Fig. 4, C and E); ATM siRNA only reduced the levels of γ-H2AX and marginally eased telomere shortening in the SAL-treated cells (Fig. 4, B and E). The data suggested that ATR was likely to play a more crucial role than ATM in the cellular response to SAL-elicited DNA damage, especially to SAL-induced telomere erosion. However, both kinases may be required for the cellular response to SAL-elicited DNA damage.

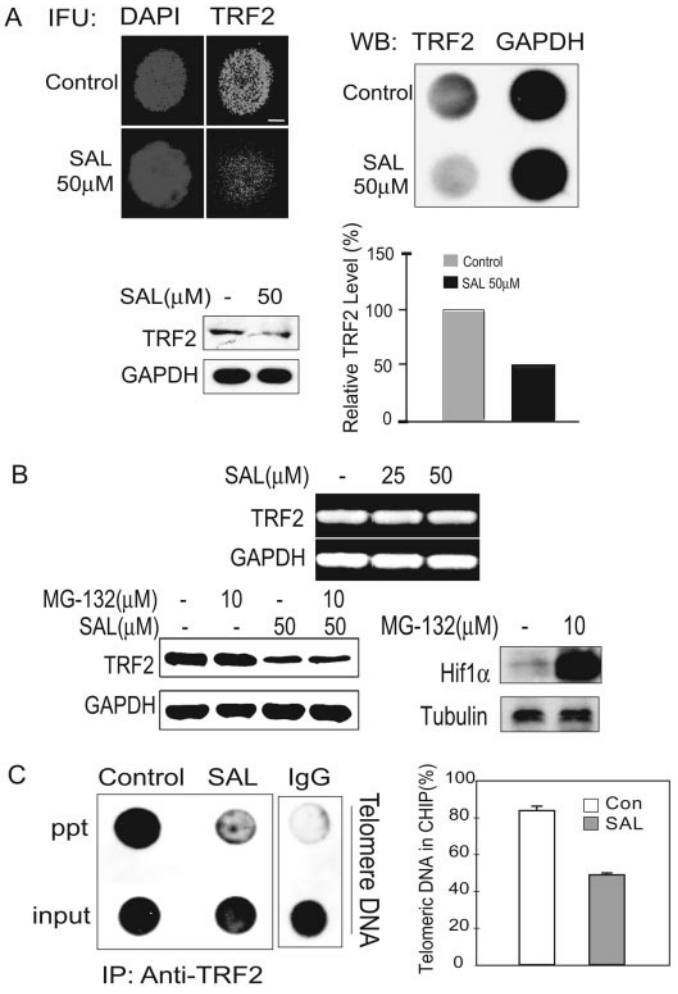

Fig. 2. SAL disrupts TRF2 protein in A549 cells. A, reduction of TRF2 protein by SAL. A549 cells were exposed to 50 μM SAL for 3 h and then subjected to immunofluorescence confocal microscopy (left, bar = 4 μm), dot blotting (right), and Western blotting (bottom). Glyceraldehyde-3-phosphate dehydrogenase was used as the loading control. Quantification for the Western blotting data were done with Adobe Photoshop 7.0.1. B, SAL-induced reduction of TRF2 protein was independent of the expression of TRF2 mRNA (top) and the degradation of TRF2 protein via the proteasome pathway (bottom). The levels of TRF2 mRNA were analyzed by RT-PCR. To detect the degradation of TRF2 protein via the proteasome pathway, A549 cells were treated with 50 μM SAL for 3 h after pre-exposure to 10 μM MG-132 for 1 h and then subjected to Western blotting to detect TRF2 (bottom left) and hypoxia-induction factor 1α (bottom right) protein level. C, reduction of the telomeric DNA bound to by TRF2. Telomere-ChIP assays were performed using a TRF2 antibody to examine the telomeric DNA bound to by TRF2. Top, telomeric DNA signals were detected with the DIG-labeled telomere probe from the Roche TeloTAGGG telomere detection system. Input, supernatant before immunoprecipitation; ppt, protein-DNA immunoprecipitate complex. Normal mouse IgG was used as the negative control. Bottom, telomere signals were semiquantitated with InGenius Bio-Imaging System. Telomeric DNA in ChIP (%) = Telomeric DNA signals of ppt/Telomeric DNA signals of input × 100%.

TRF2 Knockdown Potentiated ATR Activation, and ATR Knockdown Prevents the TRF2 Reduction after Treatment with SAL. The data above showed that TRF2 reduction was involved in DNA damage events induced by SAL and that ATR was a critical factor for both DSBs and telomeric erosion elicited by SAL. To investigate how TRF2 protein is involved in DNA damage events, we studied the relationship between TRF2 and ATR. First, we examined the change of ATR activity after TRF2 knockdown. In the mock siRNA group, SAL enhanced the ATR activity by approximately 1.0-fold. We were surprised to find that TRF2 knockdown by siRNA led to an additional 0.4-fold increment in the ATR activity in response to the SAL treatment (Fig. 5A). We then investigated the effect of ATR knockdown on TRF2 loss induced by SAL. The immunofluorescence of TRF2 showed that ATR knockdown by siRNA unexpectedly rescued the loss of TRF2 protein resulted from the treatment with SAL (Fig. 5B). These data suggested that there might be a close relationship of mutual regulation between the protein TRF2 and the kinase ATR, which is worthy of being studied further.

Discussion

We reported previously that SAL elicited DNA DSBs (Meng and Ding, 2001; Meng et al., 2001a,b; Lu et al., 2005a) and telomere erosion (Liu et al., 2004) in separate systems. In the present study, using a single system in which SAL did not induce early apoptosis (data not shown), we found that there exists a common cellular response mechanism to both DNA DSBs and telomere erosion in SAL-initiated events (i.e., SAL concurrently elicited both genomic DNA DSBs and telomere erosion in A549 cells). Further studies highlight that this dual action, driven by SAL, was in a TRF2-involved and ATR-mediated manner.

In tumor cells, the telomere length depends on the activity of telomerase, which functions mainly in S-phase during DNA replication. If the telomerase activity was inhibited, telomere would shorten in the subsequent cell cycles, which would be a long-term event. The other reason for telomere shortening is breakage in telomere DNA, which can result from oxidative damage (von Zglinicki et al., 2000). Although

SAL inhibited telomerase activity after short-term treatment, it is obviously not the main factor to shorten telomere within 3 h (Liu et al., 2004). Moreover, the colocalization of DNA damage signals and telomere signals showed that the DNA damage signals at the sites of telomeres increased with the concentrations of SAL (Fig. 1C), suggesting that the main reason for the rapid telomeric DNA loss induced by SAL could result from the DNA breakage inside telomere structure. Any telomere dysfunction resulting from mutation of telomere binding proteins, telomerase inhibition, and destruction of telomere structure would induce end-to-end fusion of chromosomes in tumor cells. Abnormal chromosomes as a result of telomere dysfunction would be harmful to the whole genome and would activate DNA damage checkpoints, which would activate apoptosis and inhibit cellular proliferation (Lechel et al., 2005; Farazi et al., 2006; Herbig and Sedivy, 2006). Therefore, telomere erosion elicited by SAL in short time might be one important reason for the final fate of tumor cells, such as proliferation inhibition and apoptosis under SAL treatment (Qing et al., 1999; Liu et al., 2004, 2005a).

TRF2 is an important telomere binding protein; its deletion or mutation leads to the loss of the telomeric 3′-tail and fusion of chromosome ends (van Steensel et al., 1998; Smogorzewska and de Lange, 2002; Klapper et al., 2003; Wang et al., 2004; Lechel et al., 2005; Li et al., 2005). TRF2 overexpression attenuates the ionizing irradiation-initiated DNA damage response to DSBs and inhibits the ionizing irradiation-induced cell cycle arrest in primary human fibroblasts (Karlseder et al., 2004; Bradshaw et al., 2005). In our study, by either overexpression of wild-type or mutated TRF2 or knockdown of TRF2 with its specific siRNAs, we demonstrate that TRF2 protects telomeric and nontelomeric DNA from SAL-induced damage (Fig. 3). In addition to its protective impact on telomere structure (Griffith et al., 1999; Yoshimura et al., 2004), TRF2 is also implicated in DNA damage and DNA repair systems (Zhu et al., 2000; Karlseder et al., 2004; Bradshaw et al., 2005; Tanaka et al., 2005; Muf-

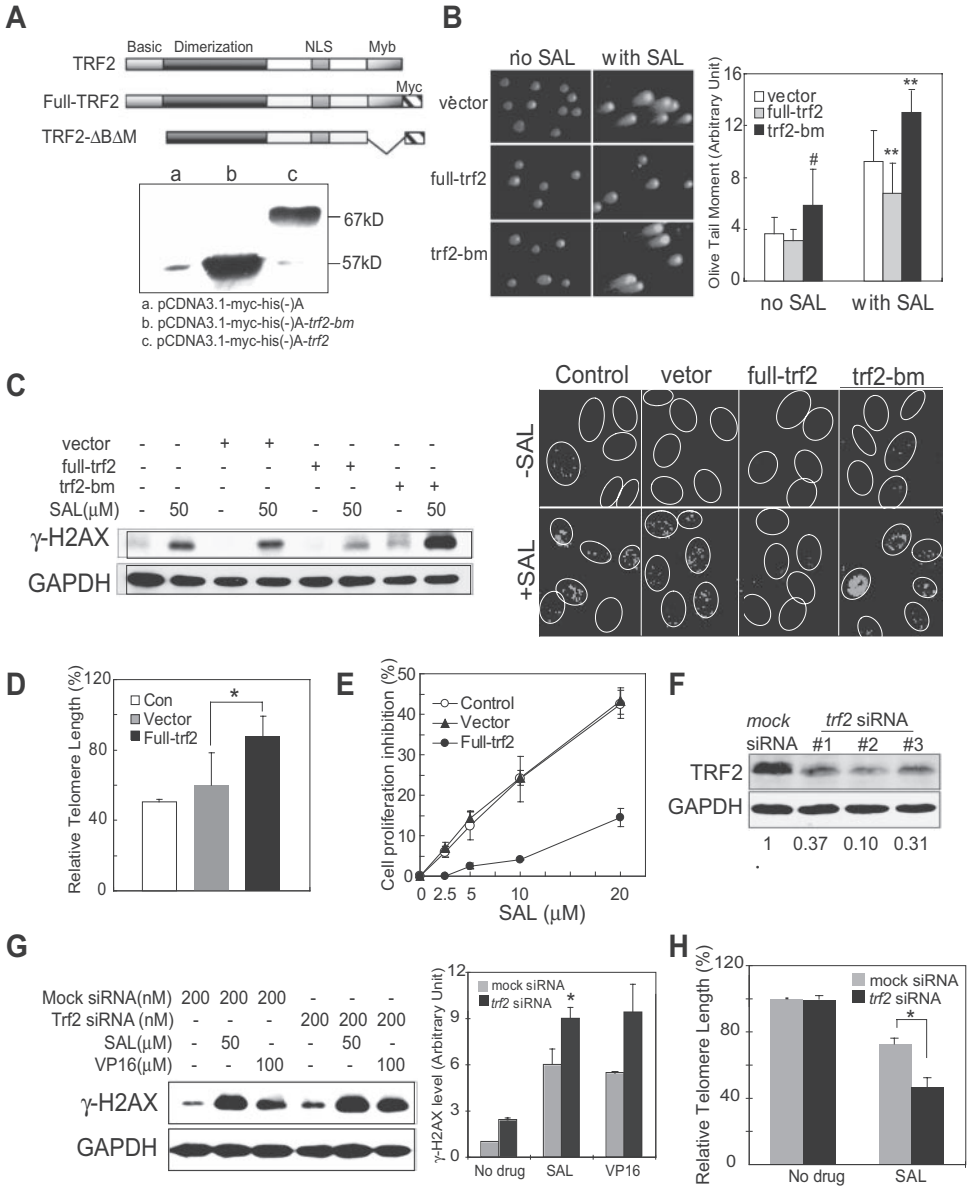

Fig. 3. TRF2 attenuates SAL-induced DNA damage and telomere erosion. A, overexpression of TRF2. Top, schematic diagrams of human TRF2 and the predicted products of different Myc-tagged *trf2* alleles. Bottom, Myc-tagged TRF2 proteins detected by Western blotting in total cell extracts from the monoclonal A549 cell population surviving over G418 selection after transfection. B, TRF2 overexpression decreased the SAL-induced DSBs examined by neutral gel electrophoresis assays. (#, $P < 0.01$ versus vector without SAL group; **, $P < 0.01$ versus vector with SAL group). C, reduced generation of γ-H2AX by SAL in TRF2 overexpressed cells examined by Western blotting (left) and by confocal microscopy (right). D, TRF2 overexpression prevented SAL-elicited telomere shortening. Telomere fluorescent signals of the groups without SAL treatment were taken as 100%. Relative telomere length of the corresponding SAL-treated groups was calculated as the ratio of their fluorescence to that of their counterpart. The results were expressed as means ± S.D., $n = 3$ (*, $P < 0.05$). E, TRF2 overexpression protected cells from SAL's cytotoxicity measured by sulforhodamine B assays. F, TRF2 knockdown 24 h after transfection with 200 nM siRNAs with different sequences. The relative density of bands was analyzed with InGenius Bio-Imaging System. G, TRF2 down-regulation enhanced the production of γ-H2AX by the SAL treatment. A549 cells were transfected with 200 nM siRNA for 24 h followed by the exposure to 50 μM SAL or 100 μM VP16 for 3 h. Western blotting was done to test the levels of γ-H2AX. H, TRF2 knockdown aggravated the telomere shortening elicited by SAL. Telomere fluorescence signals in the mock siRNA group without SAL were taken as 100%.

tuoglu et al., 2006). In fact, TRF2 is capable of being translocated to ionizing irradiation-produced nontelomeric DSB sites and being phosphorylated in an ATM-dependent manner (Bradshaw et al., 2005; Tanaka et al., 2005). TRF2 has been shown to interact with the MRE11/RAD50/NRE repair complex and to stimulate the activity of the repair enzyme DNA polymerase β (Zhu et al., 2000; Muftuoglu et al., 2006). Moreover, it has been reported that TRF2 is required for repair of nontelomeric DNA DSBs by homologous recombination (Mao et al., 2007). As such, we propose that the SAL-elicited TRF2 disruption might deprive the cells of protection, favoring shortening of telomere and thus aggravation of DNA damage.

The protein kinases ATM and ATR are critical for DNA damage response (McGowan and Russell, 2004). Their activation depends on the type of DNA damage. Irradiation or other extracellular stimuli that elicit DSBs usually activate ATM kinase (Shiloh, 2003). ATR has been shown to be usually activated by replication protein A-binding single strand (Zou and Elledge, 2003). However, our studies show that not only ATM but also ATR were involved in SAL-induced DNA DSBs (Fig. 4), as demonstrated that ATR could also respond to DSBs. Furthermore, our data were consistent with the recent report that both ATM and ATR are activated in response to irradiation-induced DSBs or UV-elicited DNA single-strand breaks; they activate different downstream substrates in the DNA damage-response systems (Helt et al., 2005). Therefore, the involvement of ATR in SAL-induced DSBs might be explained in that ATR phosphorylates certain substrates that cooperate with ATM in response to DSBs resulting from SAL.

Given the fact that ATM and ATR are critical for DNA damage response (McGowan and Russell, 2004), and ATM has been shown to mediate TRF2 phosphorylation (Tanaka et al., 2005), which in turn inhibits ATM activity in a direct manner (Karlseder et al., 2004; Celli and de Lange, 2005), we investigated the possibility of a mutual regulation of both ATM and ATR in TRF2-driven events. By using siRNA tools, we unexpectedly observed that only ATR, not ATM, is required for SAL-elicited telomere erosion (Fig. 4). Although further studies are needed with ATM- or ATR-deficient cell lines, these data partially suggested an alternative view in which the activation of ATR and ATM might play an unequal role, at least in part, in SAL-induced telomeric damage. The reason that ATM lacks its active commitment to the TRF2-mediated telomeric DNA damage in response to SAL remains unclear, which also deserves further investigation.

In addition, our findings that down-regulation of TRF2 by its specific siRNA led to the enhanced activation of ATR induced by SAL, together with the fact that the ATR siRNA transfection prevented the reduction of TRF2 in response to SAL treatment, suggested a mutual negative feedback be-

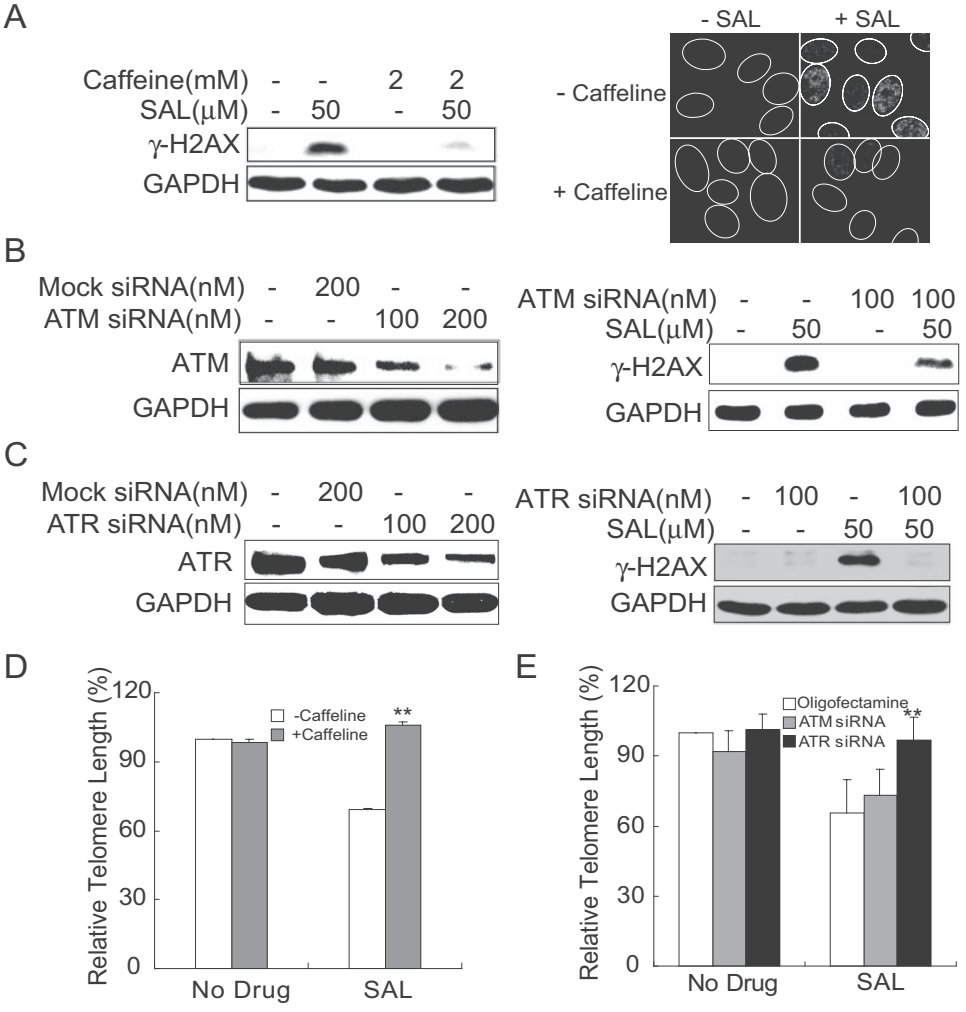

Fig. 4. ATR is required for the cellular response to the SAL-induced DNA damage and telomere shortening. A, caffeine prevented the phosphorylation of the histone H2AX. A549 cells were treated with 50 μM SAL for 3 h after the pretreatment with 2 mM caffeine for 1 h and subjected to Western blotting (left) and to immunofluorescence confocal microscopy (right). B, ATM siRNA alleviated the phosphorylation of the histone H2AX by SAL. A549 cells were transfected with 100 nM ATM siRNA for 24 h. The cells were analyzed directly for ATM expression (left) or continued to be exposed to SAL for an additional 3 h for γ-H2AX detection (right) by Western blotting. C, ATR knockdown blocked SAL-induced γ-H2AX production. After 100 nM ATR siRNA transfection for 24 h, A549 cells were analyzed directly for ATR expression (left) or continued to be exposed to SAL for an additional 3 h for γ-H2AX detection (right) by Western blotting. D, caffeine blocked the telomere shortening induced by SAL. A549 cells were treated with 50 μM SAL for 3 h after the pretreatment with 2 mM caffeine for 1 h and subjected to the relative telomere length detection as in Fig. 1D. The telomere length of the control was taken as 100%. The results were expressed as mean $\pm$ S.D., $n = 3$ (**, $p < 0.01$ versus the SAL alone-treated group). E, ATR was involved in SAL-induced telomeric length shortening. After ATM siRNA or ATR siRNA transfection as in B and C, A549 cells were exposed to 50 μM SAL for an additional 3 h. The relative telomere length was analyzed and expressed as in D (**, $P < 0.01$ versus the SAL alone-treated group).

tween the active ATR and TRF2 in tumor development. We propose that there are two possible mechanisms for the interaction between ATR and TRF2. The first is that TRF2 might inhibit ATM activation (Karlseder et al., 2004; Denchi and de Lange, 2007), because ATM could regulate upstream ATR activation (Yoo et al., 2007); consequently, TRF2 indirectly induces ATR repression. The other possible mechanism is that ATR might regulate the expression of TRF2 protein, suggested to be mediated by certain cross-talk between their signal pathways. However, the detailed interaction between TRF2 and ATR still needs to be investigated. This will go beyond the significance of SAL in cancer therapy.

In summary, SAL concurrently induces telomeric and nontelomeric DNA damage in A549 cells. The DNA damage activates the sensor kinase ATR, followed by disruption of TRF2, which in turn negatively regulates ATR activation in response to SAL. As a consequence, TRF2 reduction allows the genomic DNA and telomeres to avoid the protection related to TRF2, thus potentiating the genotoxicity and anticancer activity of SAL. This study provides the first line of evidence of TRF2 disruption in sensing DNA damage and suggests the potential mutual regulation between ATR and TRF2. With further research, it is likely that a connection between telomere maintenance and DNA damage response in cancer development will be elucidated.

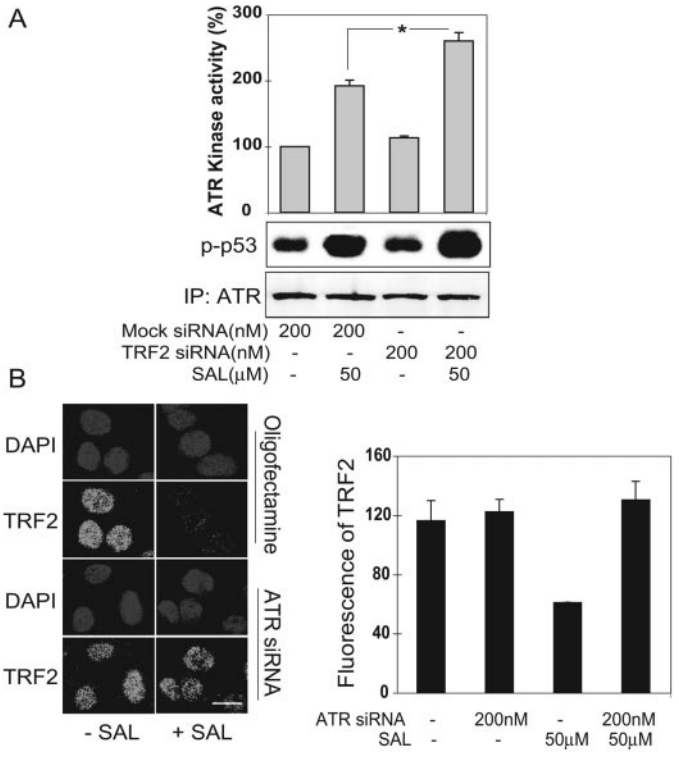

Fig. 5. TRF2 knockdown potentiates ATR activation, and ATR knockdown prevents TRF2 reduction after the treatment of SAL. A, A549 cells were transfected with 200 nM TRF2 siRNA for 24 h and then treated with 50 μM SAL for an additional 3 h. The cells were collected for ATR immunoprecipitation and in vitro ATR activity assays. Representative images of the phospho-p53 substrate detected by Western blotting were shown. Amount of phospho-p53 was semiquantitated (up). B, After 24-h transfection with 100 nM ATR siRNA, A549 cells were treated with 50 μM SAL for an additional 3 h and then subjected to immunofluorescence microscopy for TRF2 protein (left). The nuclei were stained with DAPI, bar = 4 μm. Fluorescence of TRF2 protein was semiquantitated by Photoshop 7.0 (right).

Acknowledgments

We thank Professor de Lange Titia (Rockfeller University) for the kind gift of the TRF2 expression plasmids. We thank Dr. Andrew Jobson (National Cancer Institute) for editing the manuscript.

References

Blasina A, Price BD, Turenne GA, and McGowan CH (1999) Caffeine inhibits the checkpoint kinase ATM. *Curr Biol* **9:**1135–1138.
Bradshaw PS, Stavropoulos DJ, and Meyn MS (2005) Human telomeric protein TRF2 associates with genomic double-strand breaks as an early response to DNA damage. *Nat Genet* **37:**193–197.
Canman CE, Lim DS, Cimprich KA, Taya Y, Tamai K, Sakaguchi K, Appella E, Kastan MB, and Siliciano JD (1998) Activation of the ATM kinase by ionizing radiation and phosphorylation of p53. *Science* **281:**1677–1679.
Casper AM, Nghiem P, Arlt MF, and Glover TW (2002) ATR regulates fragile site stability. *Cell* **111:**779–789.
Celli GB and de Lange T (2005) DNA processing is not required for ATM-mediated telomere damage response after TRF2 deletion. *Nat Cell Biol* **7:**712–718.
de Lange T (2005) Shelterin: the protein complex that shapes and safeguards human telomeres. *Genes Dev* **19:**2100–2110.
Denchi EL and de Lange T (2007) Protection of telomeres through independent control of ATM and ATR by TRF2 and POT1. *Nature* **448:**1068–1071.
Farazi PA, Glickman J, Horner J, and Depinho RA (2006) Cooperative interactions of p53 mutation, telomere dysfunction, and chronic liver damage in hepatocellular carcinoma progression. *Cancer Res* **66:**4766–4773.
Greider CW and Blackburn EH (1996) Telomeres, telomerase and cancer. *Sci Am* **274:**92–97.
Griffith JD, Comeau L, Rosenfield S, Stansel RM, Bianchi A, Moss H, and de Lange T (1999) Mammalian telomeres end in a large duplex loop. *Cell* **97:**503–514.
Helt CE, Cliby WA, Keng PC, Bambara RA, and O'Reilly MA (2005) Ataxia telangiectasia mutated (ATM) and ATM and Rad3-related protein exhibit selective target specificities in response to different forms of DNA damage. *J Biol Chem* **280:**1186–1192.
Herbig U and Sedivy JM (2006) Regulation of growth arrest in senescence: telomere damage is not the end of the story. *Mech Ageing Dev* **127:**16–24.
Karlseder J, Hoke K, Mirzoeva OK, Bakkenist C, Kastan MB, Petrini JH, and de Lange T (2004) The telomeric protein TRF2 binds the ATM kinase and can inhibit the ATM-dependent DNA damage response. *PLoS Biol* **2:**E240.
Klapper W, Qian W, Schulte C, and Parwaresch R (2003) DNA damage transiently increases TRF2 mRNA expression and telomerase activity. *Leukemia* **17:**2007–2015.
Lechel A, Satyanarayana A, Ju Z, Plentz RR, Schaetzlein S, Rudolph C, Wilkens L, Wiemann SU, Saretzki G, Malek NP, et al. (2005) The cellular level of telomere dysfunction determines induction of senescence or apoptosis in vivo. *EMBO Rep* **6:**275–281.
Li B, Espinal A, and Cross GA (2005) Trypanosome telomeres are protected by a homologue of mammalian TRF2. *Mol Cell Biol* **25:**5011–5021.
Li MH, Miao ZH, Tan WF, Yue JM, Zhang C, Lin LP, Zhang XW, and Ding J (2004) Pseudolaric acid B inhibits angiogenesis and reduces hypoxia-inducible factor 1alpha by promoting proteasome-mediated degradation. *Clin Cancer Res* **10:**8266–8274.
Liu WJ, Jiang JF, Xiao D, and Ding J (2002) Down-regulation of telomerase activity via protein phosphatase 2A activation in salvicine-induced human leukemia HL-60 cell apoptosis. *Biochem Pharmacol* **64:**1677–1687.
Liu WJ, Zhang YW, Shen Y, Jiang JF, Miao ZH, and Ding J (2004) Telomerase inhibition is a specific early event in salvicine-treated human lung adenocarcinoma A549 cells. *Biochem Biophys Res Commun* **323:**660–667.
Lu HR, Meng LH, Huang M, Zhu H, Miao ZH, and Ding J (2005a) DNA damage, c-myc suppression and apoptosis induced by the novel topoisomerase II inhibitor, salvicine, in human breast cancer MCF-7 cells. *Cancer Chemother Pharmacol* **55:**286–294.
Lu HR, Zhu H, Huang M, Chen Y, Cai YJ, Miao ZH, Zhang JS, and Ding J (2005b) Reactive oxygen species elicit apoptosis by concurrently disrupting topoisomerase II and DNA-dependent protein kinase. *Mol Pharmacol* **68:**983–994.
Mao Z, Seluanov A, Jiang Y, and Gorbunova V (2007) TRF2 is required for repair of nontelomeric DNA double-strand breaks by homologous recombination. *Proc Natl Acad Sci U S A* **104:**13068–13073.
McGowan CH and Russell P (2004) The DNA damage response: sensing and signaling. *Curr Opin Cell Biol* **16:**629–633.
Meng L and Ding J (2001) Induction of bulk and c-myc P2 promoter-specific DNA damage by an anti-topoisomerase II agent salvicine is an early event leading to apoptosis in HL-60 cells. *FEBS Lett* **501:**59–64.
Meng LH, He XX, Zhang JS, and Ding J (2001a) DNA topoisomerase II as the primary cellular target for salvicine in *Saccharomyces cerevisiae*. *Acta Pharmacol Sin* **22:**741–746.
Meng LH, Zhang JS, and Ding J (2001b) Salvicine, a novel DNA topoisomerase II inhibitor, exerting its effects by trapping enzyme-DNA cleavage complexes. *Biochem Pharmacol* **62:**733–741.
Muftuoglu M, Wong HK, Imam SZ, Wilson DM 3rd, Bohr VA, and Opresko PL (2006) Telomere repeat binding factor 2 interacts with base excision repair proteins and stimulates DNA synthesis by DNA polymerase beta. *Cancer Res* **66:**113–124.
Nur-E-Kamal A, Li TK, Zhang A, Qi H, Hars ES, and Liu LF (2003) Single-stranded DNA induces ataxia telangiectasia mutant (ATM)/p53-dependent DNA damage and apoptotic signals. *J Biol Chem* **278:**12475–12481.
Olive PL, Banath JP, and Durand RE (1990) Heterogeneity in radiation-induced DNA damage and repair in tumor and normal cells measured using the "comet" assay. *Radiat Res* **122:**86–94.

Qing C, Zhang JS, and Ding J (1999) In vitro cytotoxicity of salvicine, a novel diterpenoid quinone. *Zhongguo Yao Li Xue Bao* **20:**297–302.
Sarkaria JN, Busby EC, Tibbetts RS, Roos P, Taya Y, Karnitz LM, and Abraham RT (1999) Inhibition of ATM and ATR kinase activities by the radiosensitizing agent, caffeine. *Cancer Res* **59:**4375–4382.
Shiloh Y (2003) ATM and related protein kinases: safeguarding genome integrity. *Nat Rev Cancer* **3:**155–168.
Smogorzewska A and de Lange T (2002) Different telomere damage signaling pathways in human and mouse cells. *EMBO J* **21:**4338–4348.
Stansel RM, de Lange T, and Griffith JD (2001) T-loop assembly in vitro involves binding of TRF2 near the 3′ telomeric overhang. *EMBO J* **20:**5532–5540.
Tanaka H, Mendonca MS, Bradshaw PS, Hoelz DJ, Malkas LH, Meyn MS, and Gilley D (2005) DNA damage-induced phosphorylation of the human telomere-associated protein TRF2. *Proc Natl Acad Sci U S A* **102:**15539–15544.
van Steensel B, Smogorzewska A, and de Lange T (1998) TRF2 protects human telomeres from end-to-end fusions. *Cell* **92:**401–413.
von Zglinicki T, Pilger R, and Sitte N (2000) Accumulation of single-strand breaks is the major cause of telomere shortening in human fibroblasts. *Free Radic Biol Med* **28:**64–74.
Wang RC, Smogorzewska A, and de Lange T (2004) Homologous recombination generates T-loop-sized deletions at human telomeres. *Cell* **119:**355–368.
Yoo HY, Kumagai A, Shevchenko A, Shevchenko A, and Dunphy WG (2007) Ataxia-telangiectasia mutated (ATM)-dependent activation of ATR occurs through phosphorylation of TopBP1 by ATM. *J Biol Chem* **282:**17501–17506.
Yoshimura SH, Maruyama H, Ishikawa F, Ohki R, and Takeyasu K (2004) Molecular mechanisms of DNA end-loop formation by TRF2. *Genes Cells* **9:**205–218.
Zhang JS, Ding J, Tang QM, Li M, Zhao M, Lu LJ, Chen LJ, and Yuan ST (1999) Synthesis and antitumour activity of novel diterpenequinone salvicine and the analogs. *Bioorg Med Chem Lett* **9:**2731–2736.
Zhou BB, Chaturvedi P, Spring K, Scott SP, Johanson RA, Mishra R, Mattern MR, Winkler JD, and Khanna KK (2000) Caffeine abolishes the mammalian G_2/M DNA damage checkpoint by inhibiting ataxia-telangiectasia-mutated kinase activity. *J Biol Chem* **275:**10342–10348.
Zhu XD, Kuster B, Mann M, Petrini JH, and de Lange T (2000) Cell-cycle-regulated association of RAD50/MRE11/NBS1 with TRF2 and human telomeres. *Nat Genet* **25:**347–352.
Zou L and Elledge SJ (2003) Sensing DNA damage through ATRIP recognition of RPA-ssDNA complexes. *Science* **300:**1542–1548.

Address correspondence to: Dr. Jian Ding, Division of Anti-Tumor Pharmacology, State Key Laboratory of Drug Research, Shanghai Institute of *Materia Medica,* Chinese Academy of Sciences, Shanghai 201203, People's Republic of China. E-mail: jding@mail.shcnc.ac.cn

MOL PHARM

Correction to "The Telomeric Protein TRF2 Is Critical for the Protection of A549 Cells from Both Telomere Erosion and DNA Double-Strand Breaks Driven by Salvicine"

In the above article [Zhang YW, Zhang ZX, Miao ZH, and Ding J (2008) *Mol Pharmacol* **73:**824–832], there is an error in Fig. 1. In panel D, the number 100 appears twice inside the figure when it should have been on the *y*-axis. The corrected figure appears below.

The authors regret this error and apologize for any confusion or inconvenience it may have caused.